High-velocity dark states in velocity-selective coherent population trapping

M. T. Widmer, M. R. Doery, M. J. Bellanca, W. F. Buell, T. H. Bergeman, and H. J. Metcalf

Physics Department, State University of New York at Stony Brook, Stony Brook, New York 11794-3800

We have observed long-lived dark states in velocity-selective coherent population trapping (VSCPT) in a one-dimensional lin-angle-lin configuration with metastable He atoms using the $J=1 \Rightarrow 1$ transition at $\lambda = 1.083$ μm. These states are characterized by two peaks in the atomic momentum distribution at $\pm Q \hbar k$ (Q = positive integer), where k is the magnitude of the optical wave vector. VSCPT states previously observed are characterized by $Q=1$, but we have observed long-lived states with $Q=2$. Optical Bloch equation calculations show that these high-velocity dark states appear at higher Q for greater light intensity.

Some of the most interesting and important topics in the field of optical control of atomic motion occur in the quantum domain. In this domain the motion is described in terms of de Broglie wave fields of massive particles, and the interactions between these fields and the optical fields result in manipulation of the atoms by optical pumping and Raman transitions. Perhaps the most spectacular example results from the accumulation of atoms in "dark states," atomic states that cannot be excited by the light field.

Some atomic states are trivially dark, that is, they cannot be excited because the light has the wrong frequency or polarization. The more interesting cases are superposition states created by coherent Raman coupling by the optical field. A very special case occurs when those states whose evolution to excitable states vanishes exactly because their external (de Broglie wave) states are characterized by a particular momentum. Such velocity-selective coherent population trapping (VSCPT) has been a subject of considerable interest [1,2] since its first demonstration by Aspect *et al.* in 1988 [3]. VSCPT is of special interest because it enables atoms to accumulate steadily in dark states, creating arbitrarily narrow peaks in the momentum distribution. This paper presents our experimental and theoretical studies of high-velocity superposition dark states that to our knowledge have not been previously observed.

Any description of the quantum nature of the atomic motion, including VSCPT, requires that the energy of such motion be included in the Hamiltonian:

$$\mathcal{H} = \mathcal{H}_{\text{atom}} + \mathcal{H}_{AL} + \mathcal{H}_{\text{KE}}. \tag{1}$$

In (1), $\mathcal{H}_{\text{atom}}$ represents the internal atomic energy, $\mathcal{H}_{AL}$ is the interaction between the atom and the laser field, and $\mathcal{H}_{\text{KE}}$ is the kinetic energy of the atom's center-of-mass motion. Such a Hamiltonian has eigenstates of not only ($\mathcal{H}_{\text{atom}} + \mathcal{H}_{AL}$), but also of $\mathcal{H}_{\text{KE}} = P^2/2M$, where P is the momentum operator. These eigenstates are therefore labeled by quantum numbers of the atomic states as well as the momentum p. The ground state, $|p_g;g\rangle$ has energy $E_g + p_g^2/2M$ that can take on a range of values. A single laser beam of wave vector $\vec{k} \equiv (2\pi/\lambda)\hat{z}$ couples this state via absorption or stimulated emission with $|p_g + 1;e\rangle$ [we measure all momenta in units of $\hbar k$ and energy in units of $E_r \equiv \hbar \omega_r = (\hbar k)^2/2M$]. A

doublet structure caused by this coupling was first observed in 1976 in saturated absorption spectroscopy of CH_4 [4].

For a single linearly polarized light beam driving a $J=1 \Rightarrow 1$ transition, there is always a dark state corresponding to the forbidden $m_z = 0 \Rightarrow 0$ transition, even if we choose a z axis parallel to the beam's $\vec{k}$ vector. In this case the light induces only $\Delta m_z = \pm 1$ transitions because it has no π component, and for $J=1 \Rightarrow 1$, such light mixes $|p_g;m_z\rangle = |p_g;+1_g\rangle$ with $|p_g;-1_g\rangle$ via $|p_g+1;0_e\rangle$ to form two new states, ψ_L and ψ_D (L denotes light and D dark). The superposition state ψ_D is dark because $\mathcal{H}_{AL}\psi_D = 0$. We define a coordinate system such that this beam is polarized in the vertical ($\hat{x}$) direction, and propagates in the $+\hat{z}$ direction, and denote the dark states by $\psi_D = |p_g;v\rangle$ [5]. For a counterpropagating, horizontally ($\hat{y}$) polarized beam, we label the corresponding dark state $|p_g;h\rangle$. We note that the orthogonal states $|p_g;v\rangle$ and $|p_g;h\rangle$ have m_x and $m_y = 0$, respectively. They can be written in terms of the $|p;m_z\rangle$ basis as

$$|p_g;v\rangle = (|p_g;+1_g\rangle + |p_g;-1_g\rangle)/\sqrt{2},$$
$$|p_g;h\rangle = (|p_g;+1_g\rangle - |p_g;-1_g\rangle)/i\sqrt{2}. \tag{2}$$

States such as $|p_g;h\rangle$ and $|p_g;v\rangle$ cannot be dark to a beam of a second polarization. However, counterpropagating horizontally and vertically polarized beams (lin-perp-lin) can produce a dark state by coupling two states $|p_g;v\rangle$ and $|p_g';h\rangle$ whose momenta differ by ± 2. The average momentum of these two states is the family momentum $\mathbb{P}$, the momentum of the excited state coupled to each of them. The state $|p_g;v\rangle = |\mathbb{P}+1;v\rangle$ can be excited by only the horizontally polarized beam (traveling in the negative $\hat{z}$ direction) so the atomic momentum is decreased, and correspondingly for $|\mathbb{P}-1;h\rangle$ with the vertically polarized beam. Thus we can always find a value of ϕ such that the superposition $|NC(\mathbb{P})\rangle \equiv (1/\sqrt{2})[|\mathbb{P}+1;v\rangle + e^{i\phi}|\mathbb{P}-1;h\rangle]$ is dark, independent of $\mathbb{P}$; for the electric field described above, we have $\phi = 0$. Atoms cannot be transferred out of the family of three states, $|\mathbb{P}+1;v\rangle$, $|\mathbb{P};0_e\rangle$, and $|\mathbb{P}-1;h\rangle$ except by spontaneous emission, and the family is called closed [1].

Such a superposition $|NC(\mathbb{P})\rangle$ is a stationary state if $(\mathbb{P}+1)^2 = (\mathbb{P}-1)^2$ which requires $\mathbb{P}=0$. Then $|NC(\mathbb{P}=0)\rangle$ is an eigenstate of the kinetic energy term $P^2/2M$ in the Hamiltonian as well as the atomic and atom-laser interaction terms.

For $\mathbb{P} \neq 0$, $|NC(\mathbb{P})\rangle$ is not an eigenstate of $\mathscr{H}_{\mathrm{KE}}$ so the atomic wave function, which is initially $|NC(\mathbb{P})\rangle$, evolves into a superposition of $|NC(\mathbb{P})\rangle$ and $|C(\mathbb{P})\rangle$ $\equiv [|\mathbb{P}+1;v\rangle - e^{i\phi}|\mathbb{P}-1;h\rangle]/\sqrt{2}$. Unlike $|NC(\mathbb{P})\rangle$, $|C(\mathbb{P})\rangle$ can be excited to $|\mathbb{P};0_e\rangle$ by the light. Subsequent spontaneous emission from $|\mathbb{P};0_e\rangle$ then results in transitions to other families. As a result, atoms with $\mathbb{P} \neq 0$ continue to interact with the light field until they are optically pumped via a random walk in momentum space into the dark eigenstate $|NC(0)\rangle$; at this point the interaction ceases and $|NC(0)\rangle$ is therefore called a trapped state. Measuring the momentum distribution of an ensemble of atoms in $|NC(0)\rangle$ results in two distinct peaks at $p_g = \pm 1$; this is the usual VSCPT as first observed by Aspect *et al.* [3].

We now consider two linearly polarized counterpropagating beams with their electric fields at an angle θ to one another, as discussed by many authors [6–9]; Figure 1 shows the resulting configuration (one beam is vertically polarized). The state $|p_g;v\rangle$ is still dark to this vertically polarized beam, but it is no longer orthogonal to the state that is dark to the other beam, $|p_g';\theta\rangle = [e^{-i\theta}|\mathbb{P}-1;+1_g\rangle + e^{i\theta}|\mathbb{P}-1;-1_g\rangle]/\sqrt{2}$. Nevertheless, there is a dark state superposition $|NC(\mathbb{P};\theta)\rangle = [|\mathbb{P}-1;\theta\rangle + |\mathbb{P}+1;v\rangle]/\sqrt{2}$ $(p_g = p_g'+2 = \mathbb{P}+1)$, but the components of the superposition are not part of a closed family. Such superposition states offer new insights into VSCPT and related phenomena. Again, $|NC(\mathbb{P};\theta)\rangle$ is an eigenstate of the Hamiltonian only for $\mathbb{P}=0$.

The lin-angle-lin optical field described above can couple, and thus produce superpositions of the two states $|NC(\pm 1;\theta)\rangle$ that have the same average energy. We find
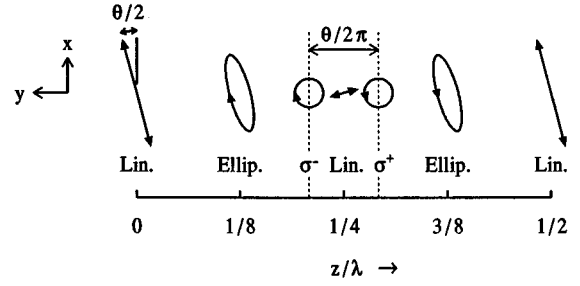
FIG. 1. The polarization scheme for counterpropagating beams linearly polarized at angle θ to one another. Unlike the more familiar case for $\theta = 90°$, here the amplitudes of the horizontal and vertical linear polarizations are unequal as indicated, the oppositely circularly polarized regions have a very small amplitude, and their separation is not $\lambda/4$.

$$|NC^{(2)}(\mathbb{P}^{(2)}=0);\theta\rangle \equiv [|NC(-1;\theta)\rangle$$
$$- |NC(+1;\theta)\rangle]/\{2-\cos(\theta)\}^{1/2}, \quad (3)$$

where $\mathbb{P}^{(2)}$ is the average of the family momenta of the superposition. The momentum distributions of $|NC(\pm 1;\theta)\rangle$ consist of δ functions at $p_g = 0, \pm 2$ so their superposition results in three peaks.

The relative phase of the superposition in (3) is chosen to be π because this allows near cancellation of the peak at $p_g = 0$, leaving just the two peaks at $p_g = \pm 2$. This is easily seen by expanding $|NC^{(2)}\rangle$ in the basis $|p;m_z\rangle$:

$$|NC^{(2)}\rangle = \{e^{i\theta}|-2;-1_g\rangle + e^{-i\theta}|-2;+1_g\rangle - |2;-1_g\rangle - |2;+1_g\rangle + (1-e^{i\theta})[|0;-1_g\rangle - e^{-i\theta}|0;+1_g\rangle]\}/2\{2-\cos(\theta)\}^{1/2}.$$
$$(4)$$

For small θ, we note that the major contribution to $|NC^{(2)}\rangle$ is from the momentum components at ± 2 because the relative contributions to the momentum distribution from states with $p_g = 0$ is proportional to $|1-e^{i\theta}|^2 \sim \theta^2$. Even though the two nonstationary states $|NC(\pm 1)\rangle$ may each be readily pumped to the excited state through their motional mixing with $|C(\pm 1)\rangle$, for small θ the state $|NC^{(2)}(0;\theta)\rangle$ has a far lower mixing rate because it is nearly an eigenstate having kinetic energy $\cong 4\hbar\omega_r$. Exact cancellation of the $p=0$ component is only possible for $\theta = 0$, but that case has a velocity-independent dark state.

The idea of high-velocity dark states such as $|NC^{(2)}\rangle$ may be generalized as illustrated in Fig. 2. By superposition of the Q states $|NC(\mathbb{P}_n)\rangle$, where $\mathbb{P}_n = \mathbb{P}_{n-1}+2$ and $n = -Q+1, -Q+3,...,Q-1$, one may obtain near cancellation of the intermediate velocities to produce a state $|NC^{(Q)}\rangle$ composed almost entirely of momenta at $\pm Q$; Fig. 2 illustrates the case of $Q=4$.

In the laser field that produces population in $|NC^{(2)}\rangle$, the state $|NC(0)\rangle$ is a perfect trapping state, and population accumulated in it produces the well-known peaks in the momentum distribution at ± 1 [1–3]. In addition, because popu-

lation also accumulates in $|NC^{(2)}\rangle$, the momentum distribution will have peaks at ± 2 [8]. Both of these long-lived states are populated by a random walk in momentum space, and each of them has a lifetime longer than the experimental interaction time. Thus there are four very narrow
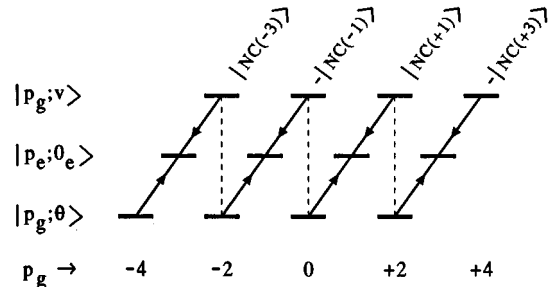
FIG. 2. The transition scheme for $Q=4$. The nonorthogonal states that comprise the superposition are denoted by v and θ, and the various ground-state momentum values are indicated. The index n corresponds to $\mathbb{P}$, the odd-integer, excited-state momenta.
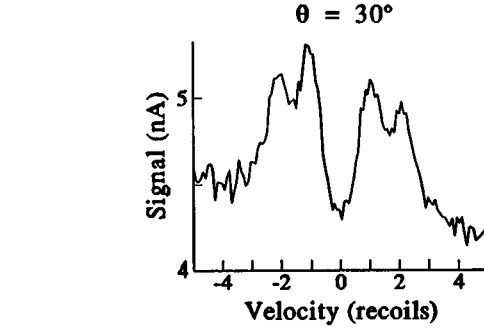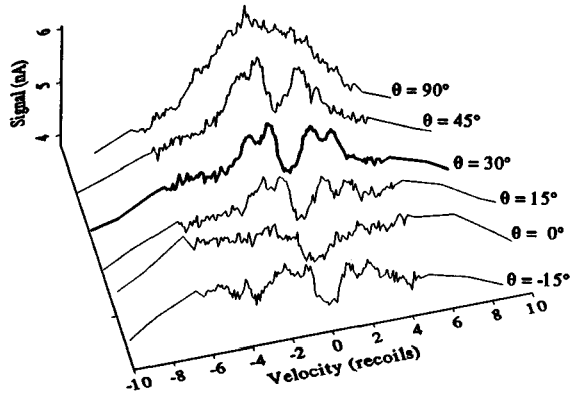
FIG. 3. Measured velocity distributions after 20 μs interaction time for $s=9.5$, $\delta=0$ for various angles θ. The inset is for $\theta=30°$ where the four-peaked structure is most evident.

(full width at half maximum $\leq \hbar k$) peaks expected in the measured momentum distribution. We have observed such distributions in triple metastable helium (He*) driven by light of wavelength $\lambda=1.083$ μm (see Fig. 3).

Our apparatus has been previously described [10,11], but is briefly reviewed here. A narrow beam of He* crosses the counterpropagating laser beams at 90° in a region where the magnetic field is carefully nulled to below 5 mG. It travels 1.8 m to a movable detector covered by a narrow slit that measures the atomic spatial distribution. The momentum distribution is derived from this spatial distribution and the experimental geometry with a resolution of better than 0.5$\hbar k$.

Figure 3 shows measured velocity distributions for $s=9.5$ and $\delta=0$ for a series of angles θ. Here $s \equiv I/I_{sat}$, $I_{sat} \equiv \pi h c/3\lambda^3 \tau = 0.17$ mW/cm^2 is the saturation intensity for the He* transition, I is the intensity of one laser beam, and $\tau=98$ ns is the natural lifetime of the excited states. For $\theta=90°$ at such high intensity and zero detuning, VSCPT has

little velocity selectivity. As θ is decreased the characteristic VSCPT peaks at $p_g=\pm 1$ become evident, as well as higher-order peaks at $p_g=\pm 2$. The inset highlights the velocity distribution for $\theta=30°$ where the multipeak structure is most pronounced. As θ is decreased further, the efficiency of VSCPT decreases (proportional to $\sin(\theta)$ [6]). Finally, at $\theta=0$ the dark state is completely velocity independent, although our calculations show some weak structure.

We have employed two independent quantitative methods to describe our experiments. In one, we diagonalize the Hamiltonian matrix for the ground states $m_z=\pm 1$ and the excited state $m_z=0$ with 100–1000 momentum values for the atomic KE. The spontaneous decay is given by the imaginary part of a complex energy for the excited state, thus making the matrix non-Hermitian [8]. The resulting complex eigenvalues combine both internal and external energies; those with smallest imaginary parts correspond to the longest lifetimes and are nearly dark (gray). Figure 4 shows clearly that
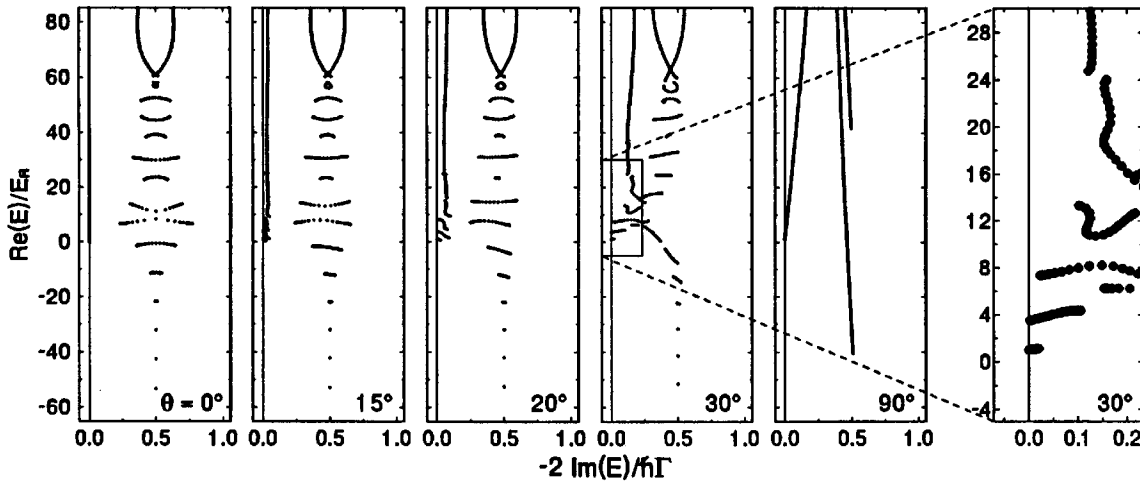
FIG. 4. Real vs imaginary parts of the energies calculated by matrix diagonalization for several angles θ. We used $s=10$ and $\delta=0$. A small imaginary part $|\text{Im}(E)|$ corresponds to a long lifetime: trapped states have $|\text{Im}(E)|=0$. Note the development of the dark states with increasing θ from the forbidden $m=0 \Rightarrow 0$ transition that is dark for all $\text{Re}(E)$ at $\theta=0$. Also note the absence of band structure at $\theta=90°$. An enlarged view of a small region for $\theta=30°$ is also shown. $\text{Re}(E)$ at minimum $|\text{Im}(E)|$ differ slightly from 1, 4, and 9 because these eigenstates are not perfectly dark and thus have a nonzero light shift.

there are long-lived states near energies $1\hbar\omega_r$, $4\hbar\omega_r$, and $9\hbar\omega_r$, corresponding to $Q=1$, 2, and 3. The energy gaps in Fig. 4 correspond to allowed and forbidden bands that arise from the periodic potential associated with the spatially dependent light shift (whose amplitude vanishes for $\theta=\pi/2$). The gray and dark states appear at either the band edge or center, depending on whether Q is odd or even.

In the other method we calculate the temporal evolution of the density matrix using a basis of direct products of internal atomic states with free particle momentum states ranging up to several times $\hbar k$. The Hamiltonian for this fully quantized calculation includes the center-of-mass atomic motion as well as the atomic states and the laser-atom interaction [12,13]. This method can be applied to light fields of arbitrary intensity and polarization configurations, as well as to atoms with arbitrary angular momentum schemes. It has the advantage of providing information about the time development of the momentum distribution, and allowing us to model the passage of atoms through inhomogeneous light fields. The evolution of the momentum distribution for several laser configurations is shown in Fig. 5. It is clear that the $Q=2$ peaks are present for small θ, and at higher intensities the higher Q peaks also appear.

These calculations suggest that higher intensities lead to population of gray states with higher values of Q. This conclusion is intuitively satisfying because coherence between momentum families is established by Raman couplings of order $2Q$, and the strength of such nonlinear processes clearly increases with intensity. We might even guess that the coupling matrix element (Rabi frequency Ω_R) required to observe such Raman couplings of order Q must be large compared to the KE matrix elements on the diagonal of the Hamiltonian, which are $p^2/2M \lesssim Q^2\hbar\omega_r$. The necessary intensity ($\propto\Omega_R^2$) thus scales as $p^4\propto Q^4$. We plan to try to observe these states, which correspond to the bound states in the dark state gauge potential [14]. Furthermore, temporarily
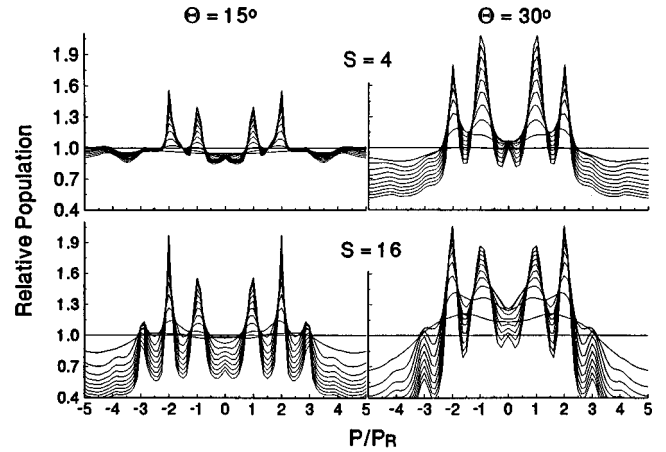
FIG. 5. Velocity distributions for $s=4$ and 16, $\theta=15°$ and 30°, and $\delta=0$ as calculated using the quantum density matrix method (see Ref. [12]). Note the small peaks at $p_g=0$ and $\theta=15°$, and slightly larger ones for $\theta=30°$. All populations begin at unity (flat line), and the evolution for each 2 μs interval is shown for a total of 20 μs, corresponding to the experimental interaction time.

trapping population in dark states of high p inhibits the laser cooling process, thus suggesting that this picture provides an alternate view of the linear scaling of the limit of Sisyphus cooling with intensity. We are presently investigating this new idea.

In summary, we have presented our study of previously unobserved ground states with long lifetimes resulting from near cancellation of optical excitation amplitudes. These result from coherences between states whose momenta differ by more than ± 2 that are coupled by Raman transitions of order higher than 2.

[1] A. Aspect *et al.*, J. Opt. Soc. Am. B **6**, 2112 (1989).
[2] F. Bardou *et al.*, Phys. Rev. Lett. **72**, 203 (1994).
[3] A. Aspect *et al.*, Phys. Rev. Lett. **61**, 826 (1988).
[4] J. L. Hall *et al.*, Phys. Rev. Lett. **37**, 1339 (1976).
[5] F. Mauri and E. Arimondo, Europhys. Lett. **16**, 717 (1991).
[6] M. Shahriar *et al.*, Opt. Commun. **103**, 453 (1993).
[7] M. Shahriar *et al.*, Phys. Rev. A **48**, R4035 (1993).
[8] P. Marte *et al.*, Phys. Rev. A **49**, 4826 (1994).
[9] M. Weidemüller *et al.*, Europhys. Lett. **27**, 109 (1994).
[10] M. Doery *et al.*, Phys. Rev. Lett. **72**, 2546 (1994).
[11] T. Chuang and H. J. Metcalf, Appl. Opt. **30**, 2495 (1991).
[12] M. R. Doery *et al.*, Phys. Rev. A **52**, 2295 (1995).
[13] M. R. Doery *et al.*, Phys. Rev. A **51**, 4881 (1995); T. Bergeman, Phys. Rev. A **48**, R3425 (1993).
[14] R. Dum and M. Olshanii (private communication).